Structure of evaporated pure amorphous silicon: Neutron-diffraction and reverse Monte Carlo investigations

S. Kugler

Quantum Theory Group, Institute of Physics, Technical University of Budapest, H-1521 Budapest, Hungary

L. Pusztai

Laboratory of Theoretical Chemistry, Lorand Eötvös University, H-1518 Budapest 112, Pf 32, Hungary

L. Rosta

Central Research Institute for Physics, H-1525 Budapest, Pf 49, Hungary

P. Chieux

Institut Laue-Langevin, 156 X, F-38042 Grenoble CEDEX, France

R. Bellissent

Laboratoire Léon Brillouin, Centre d'Etudes Nucléaires de Saclay, 91191 Gif-sur-Yvette Cedex, France

A neutron-diffraction measurement in the 0–23 Å^{-1} inverse space interval was performed on pure amorphous Si. With the structure factor obtained experimentally three-dimensional models were constructed by reverse Monte Carlo simulation for the determination of the atomic structure of a-Si. The radial distribution function was calculated directly from the large-scale models and was derived traditionally from these wide range spectra, as well.

There is considerable interest in the determination of the microscopic structure of pure amorphous silicon. It has received particular attention since the material is covalently bonded and serves as the best prototype of disordered solids. Some experimental structural studies have been made on a-Si using electron diffraction[1,2] and x-ray absorption,[3] but still the neutron-diffraction technique gives the most accessible information on the structure, provided that the quantity of the sample is sufficient. Recently three different measurements using neutron-diffraction methods[4–6] have been published.

Numerous handbuilt and computer-generated models[7–9] have been constructed in different ways in the last two decades. In the relaxed continuous random network models the Keating, the Stillinger-Weber, the Weber bond-charge potential, and the Lifson-Warshel force field were used as assumptions for the interatomic potential to minimize the total energy. Other models containing some threefold coordinated atoms were obtained by molecular dynamics technique. The number of atoms in the models varied from several tens to hundreds. For the lack of experimental information, pure amorphous silicon radial distribution functions (RDF's) calculated from the above theoretical models were mostly compared to neutron-diffraction data on amorphous germanium.[10] Small-angle neutron scattering[11,12] was applied to obtain additional information on the voids and larger-scale density fluctuations in the structure of a-Si.

A 0.45 g nearly pure evaporated amorphous Si sample was prepared in the Central Research Institute for Physics, Budapest. A preliminary neutron-diffraction experiment[4] was performed at the 7C2 spectrometer installed on the hot source of the reactor Orphee at Saclay. Using an incident wavelength of $\lambda = 0.706$ Å, the momentum transfer range of 0.5–16 Å^{-1} was covered. The concen-

tration of hydrogen in the sample was 1.95%. In spite of this low concentration, particular attention was paid when carrying out the inelastic correction.

The present neutron-diffraction measurement was performed using the D4 twin-axis diffractometer at the high-flux reactor in the Institut Laue-Langevin. The incident neutron wavelength of 0.4977 Å and the angular ranges of 1.5°–65° and 46°–131° covered by the two multidetectors provided us with a momentum transfer range of 0.33–23.0 Å^{-1}. Data evaluation was carried out by the classical corrections for transmission,[13] multiple scattering,[14] and inelastic scattering.[15,16] The measured structure factor of a-Si is shown in Fig. 1.

The most common characteristics of the existing models of a-Si are that they contain almost exclusively tetrahedral (109.5°) Si—Si—Si bond angles. In order to demonstrate that radically different covalent angles can also be relevant the Cambridge Structural Database[17]
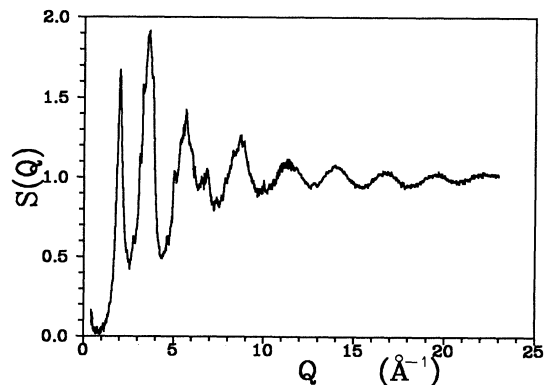

FIG. 1. Measured structure factor of pure evaporated a-Si in the range of 0–23 Å^{-1}.

(CSD) was searched for molecules containing at least one Si-Si-Si fragment. 346 suitable targets have been found. The results of this search are shown in Fig. 2. Each point represents a measured bond angle as a function of bond length. Since in one Si-Si-Si fragment two bond lengths belong to one bond angle, 692 points are plotted. The overwhelming majority of these points (about 500) fall in the appreciated region, i.e., around 2.35 Å and the tetrahedral angle. There are a few extrema, and some well-defined, unexpected regions can also be found. The first conclusion is that the Si_3 triangle is present among the fragments. The bond angles are about 60°, i.e., the triangles are nearly equilateral. Most of the theoretical models for a-Si do not contain such a part of the structure. There are a number of angles around 90°, too. The last remark on Fig. 2 is that a Si—Si—Si bond angle greater than 130° has never been encountered. Bond lengths lie between 2.29 and 2.65 Å but there are very few bonds that are longer than 2.46 Å.

Reverse Monte Carlo (RMC) simulation[18] was applied for the analysis of the diffraction data and at the same time, for modeling the structure of a-Si. This method generates three-dimensional particle configurations that are consistent with the experimental structure factor. The basic algorithm has been described elsewhere[18,19] in detail, therefore only a short summary is given here, outlining the use of constraints.

(a) Start with an initial set of Cartesian coordinates (particle configuration). Calculate its radial distribution function $g_0(r)$ and structure factor $S_0(Q)$. Calculate also χ_0^2, the difference between simulated and experimental structure factors. (b) A new (trial) configuration is generated by the random motion of a particle. (c) Check whether the new configuration satisfies the constraint(s) applied. If not, start again from (b). (This is an additional step to the standard RMC simulation.) (d) Provided that the constraints are satisfied, calculate $g_n(r), S_n(Q)$, and χ_n^2 for the new (trial) configuration. (e) If $\chi_n^2 < \chi_{n-1}^2$, the new configuration becomes the starting configuration, i.e., the move is accepted, otherwise it is accepted with a probability that follows the normal distribution. (f) Repeat the process from (b) until χ^2 converges to its "equilibrium" value. In this way, sets of particle coordinates are generated that are consistent with a given diffraction
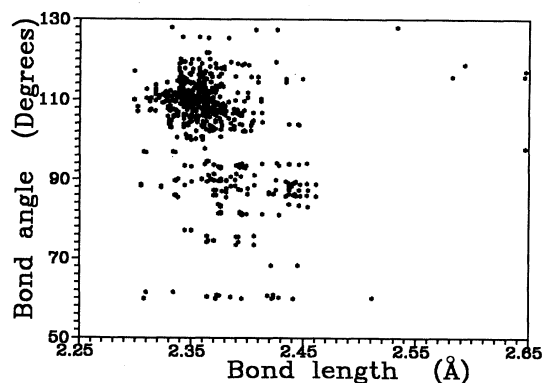

FIG. 2. Measured Si—Si—Si bond angles (deg) as a function of 692 Si—Si bond lengths (Å), obtained from the CSD.

data set *and* with the constraint(s) applied.

The first type of constraint used in our RMC simulations was one imposed on the *coordination number*. It can easily be prescribed—and implemented by a proper computer code—that a given fraction of particles *must have* strictly a given number of particles within a fixed distance. In this way even moleculelike objects can be bound together with a great flexibility in terms of bond angles.[19]

For systems where interparticle interactions are—presumably—mostly covalent, that is, where bonds are *directed*, introducing constraints on bond angles might be useful. The implementation of such constraints, however, is not trivial in disordered media, as even the definition of bond angles can be ambiguous. Throughout this study we consider any vector joining two neighbors as a bond; two bonds having a common vertex (i.e., particle) form a bond angle. In systems like a-Si it is straightforward to require that most of the angles should be roughly tetrahedral. Angles far from the tetrahedral value are less probable but permitted, as it could be concluded from the analysis of the CSD. Why should constraints be used if unconstrained RMC is able to reproduce experimental data itself? Although it was demonstrated that RMC results are sufficiently unique at higher packing fraction values and in the absence of directional forces,[20,21] it is far from guaranteed that this holds for covalent systems of relatively low packing fraction. In the latter case it is possible in principle that a range of structural models are consistent with a given diffraction data, instead of one single model. These models can most easily be manifested through *constraints* on the steric arrangement. Some constraints may not be consistent with the original diffraction data, i.e., it may not be possible to achieve the same level of agreement between model and experiment as without the constraint in question. In these cases the models attributed to these constraints should be considered as impossible, provided that the quality of the diffraction data is good enough.

For the three structural models which are going to be discussed in this work (see below) identical basic parameters were used. In all cases $N = 1728$ particles (i.e., points) were confined in a cubic box of sides $L = 32$ Å. This setup gave the experimental microscopic number density of $\rho = 0.0505$ Å^{-3}. The experimentally measured and corrected structure factor was used as input data for the RMC calculations. A hard-core diameter (lowest limit of bond length) of 2.20 Å was also applied in order to efficiently avoid physically meaningless configurations. In all three runs $\sim 10^6$ accepted steps were completed.

Of the three calculations, the first one (referred as model 1) is the result of an unconstrained RMC, i.e., that of a calculation without item (c) (see the algorithm above). Model 2 was produced using a constraint on coordination number: every atom in the configuration was required to have exactly four neighbors in the first coordination shell. The boundary for this shell was set at 2.7 Å, where the $g(r)$ function has almost reached its first minimum. The second reason for selecting this value was that there was no Si—Si bond longer than 2.65 Å found in any compound. Model 3 satisfies the most complicated constraint

applied during this study. Here also it was required that all the atoms have four neighbors. As an addition to this, if an attempted move resulted in newly formed bond angles with an average that did not fit in a normal-like distribution centered around the tetrahedral angle, the move was immediately rejected. The σ parameter of the distribution was fixed at $\sigma = 0.08$. Smaller values (i.e., more strict constraints) caused bottlenecks in the simulation course.

Figure 3(a) shows the comparison of the RMC solution for model 1 and the experimental $S(Q)$. The overall agreement is good, but several attempts were made for improving the picture even further. It is thought that the greater amplitude of the oscillations at higher Q values and the small-angle scattering part of the $S(Q)$ curve could be fitted more successfully using a much bigger box, as in highly ordered systems truncation effects are important. Figure 3(b) gives the same comparison for model 3. [The fit for model 2 is undistinguishable from Fig. 3(a) so it is not shown here.] We consider model 3 as the best model out of the three on the basis of $S(Q)$ fits.

The RDF was calculated for the models and was also derived as the sine Fourier transform of the measured $S(Q)$. The RDF for model 1 (identical to model 2) is displayed in Fig. 4(a); model 3 is given in Fig. 4(b). Figure 4(c) contains the traditionally evaluated $g(r)$. The characteristics of these functions are rather similar, the full widths of the first neighbor peaks being different at half maximum.
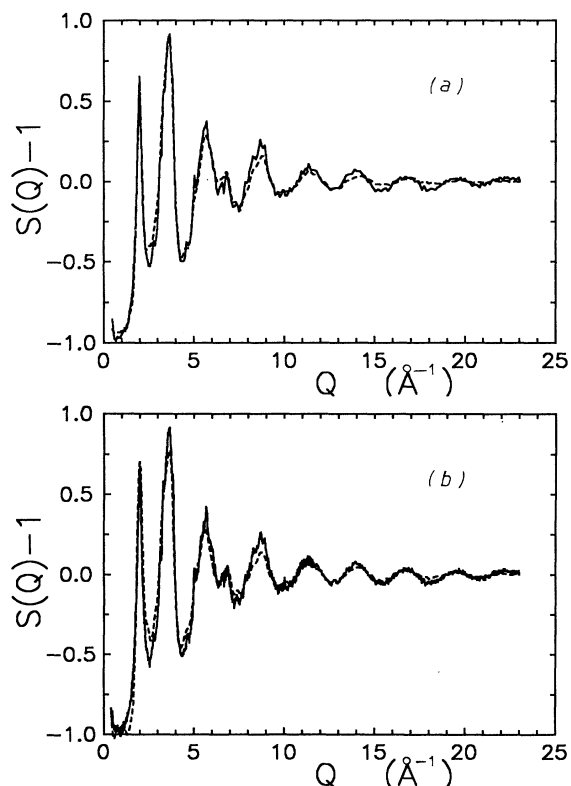
In order to resolve these small differences, it is clear that very high accuracy diffraction experiments will be necessary as well as the use of methods for comparing the models to the experimental results. This is beyond the scope of the present study.

However, cosine distribution of bond angles, $B(\cos\Theta)$, easily shows the difference between the three microscopic structures obtained by three different constraints (Fig. 5). Model 1 gives results strikingly different from that of the other two models, in terms of $B(\cos\Theta)$. The cosine distribution for model 1 has a large peak at around 55–60°, and also, a large proportion of angles were found near 180° (see Fig. 5). These two features are in contrast with a number of assumptions based on, for example, conductivity measurements which suggest that in amorphous Si

FIG. 3. Measured structure factor (solid line) compared to RMC models in the range of 0–23 Å^{-1}. Dotted lines: (a) models 1 and 2; and (b) model 3.
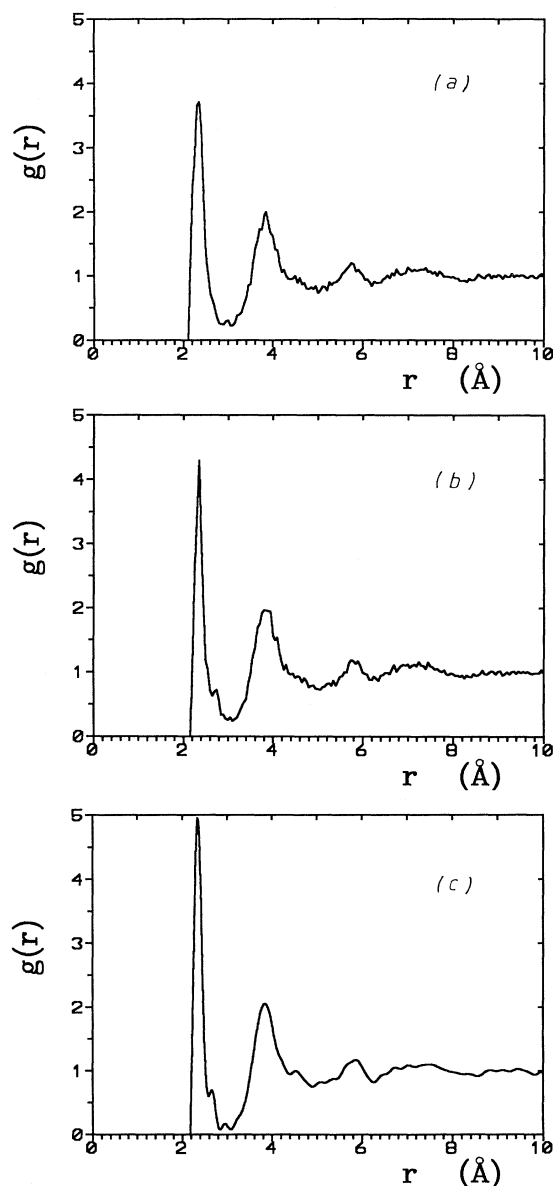
FIG. 4. $g(r)$ function as it was derived directly from (a) models 1 and 2, (b) model 3, and (c) as it was calculated by Fourier transformation of experimental $S(Q)$.

tetrahedral angles have to be dominant. This is due to the electronic structure of covalently bound Si atoms. It was because of this strong argument that we felt necessary to try out whether it was possible to construct models which are consistent with the above assumption *and at the same time*, with the diffraction data. It should be noted, however, that the most basic feature, the strong peak around 109.5° is provided by the unconstrained model. This shows that even the presence of evidently directed bonds cannot make the simplest RMC solution totally meaningless. Model 2 reflects probably the most fundamental requirement, that atoms in any solid form of Si should be fourfold coordinated. It can be seen from Fig. 5 that this simple constraint greatly reduces the freedom of moving atoms around and yields a bond angle distribution which is roughly coherent with the above ideas. The main problem with this picture is the probable over-representation of angles higher than 130°. Model 3 was introduced in order to further narrow the cosine distribution, as it was aimed to find the structural model that gives the most exclusive presence of tetrahedral angles. As it is evident from Fig. 5, using the algorithm given in the previous section, no essential narrowing could be achieved, compared to model 2. When smaller values than 0.08 were used for the σ parameter of the normal distribution the experimental $S(Q)$ could not be fitted at the demonstrated level. We also tried simply to reject any move that would form just one single angle bigger than 150°, but this attempt also resulted in poorer agreement. In principle, it seems possible to set up more sophisticated constraint algorithms (and to use a much bigger simulation box), but computer time soon would be a prohibitive factor with no substantially new information gained.

In summary, the values of Q up to 23 Å were employed to determine the $S(Q)$ of pure amorphous silicon. Together with the Fourier transform of $S(Q)$, we have
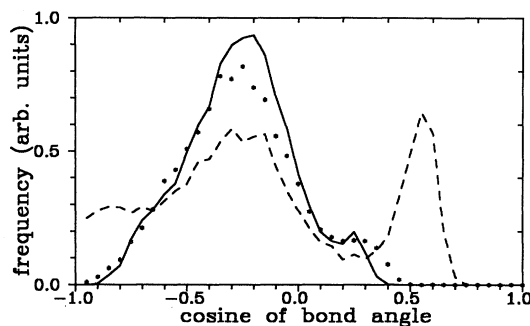

FIG. 5. Cosine distributions for the different models. (Model 1, dashed line; model 2, symbols; model 3, solid line).

presented a possibility to derive the RDF for a-Si. The method eliminates the lack of measured data beyond 23 Å and additionally, it can produce geometrical models for an amorphous material. In all our structural models for a-Si tetrahedral angles dominate the angle (or cosine) distribution, although their fraction can be noticeably different. High accuracy diffraction data and detailed quantitative comparsion with the models will be necessary to find out the most probable answer. Alternatively total energy calculations should be performed.

[1]S. C. Moss and J. F. Graczyk, in *Proceedings of the Tenth International Conference on Physics of Semiconductors, Cambridge, MA*, edited by S. P. Keller, J. C. Hesnel, and F. Stern (U.S. Atomic Energy Commission, Washington, D.C., 1970), p. 658.

[2]A. Barna, P. B. Barna, G. Radnóczi, L. Tóth, and P. Thomas, Phys. Status Solidi A **41**, 81 (1977).

[3]A. Di Cicco, A. Bianconi, C. Coluzza, P. Rudolf, P. Lagarde, A. M. Flank, and A. Marcelli, J. Non-Cryst. Solids **116**, 27 (1990).

[4]S. Kugler, G. Molnár, G. Petö, E. Zsoldos, L. Rosta, A. Menelle, and R. Bellissent, Phys. Rev. B **40**, 8030 (1989), and references therein.

[5]J. Fortner and J. S. Lannin, J. Non-Cryst. Solids **106**, 128 (1988); Phys. Rev. B **39**, 5527 (1989).

[6]R. Bellissent, A. Menelle, W. S. Howells, A. C. Wright, T. M. Brunier, R. N. Sinclair, and F. Jansen, Physica B **156&157**, 217 (1989).

[7]See Refs. 1–17 in Ref. 4.

[8]I. Stich, R. Car, and M. Parrinello, Phys. Rev. B **44**, 11 092 (1991).

[9]J. M. Holender and G. J. Morgan, J. Phys. Condens. Matter **3**,

1947 (1991).

[10]J. H. Etherington, A. C. Wright, J. T. Wenzel, J. C. Dore, J. H. Clarke, and R. N. Sinclair, J. Non-Cryst. Solids **48**, 265 (1982).

[11]R. Bellissent, J. Non-Cryst. Solids **97&98**, 329 (1987).

[12]A. Menelle, J. Non-Cryst. Solids **97&98**, 337 (1987).

[13]H. H. Paalman and C. J. Pings, J. Appl. Phys. **33**, 2635 (1962).

[14]I. A. Blech and B. L. Auerbach, Phys. Rev. A **137**, 1113 (1965).

[15]J. L. Yarnell, M. J. Katz, R. G. Wenzel, and H. S. Koening, Phys. Rev. A **7**, 2130 (1973).

[16]P. Chieux, R. de Kouchkovski, and B. Boucher, J. Phys. F **14**, 2239 (1984).

[17]F. H. Allen, O. Kennard, and R. Taylor, Acc. Chem. Res. **16**, 146 (1983).

[18]R. L. McGreevy and L. Pusztai, Molec. Sim. **1**, 369 (1988).

[19]R. L. McGreevy, M. A. Howe, D. A. Keen, and K. Clausen, IOP Conf. Ser. **107**, 164 (1991).

[20]L. Pusztai and G. Tóth, J. Chem. Phys. **94**, 3042 (1991).

[21]R. L. McGreevy and M. A. Howe, Phys. Chem. Liq. **24**, 1 (1991).